Melting and freezing of Ar in nanopores

D. Wallacher and K. Knorr
Technische Physik, Universität des Saarlandes, D-66041 Saarbrücken, Germany
(Received 24 August 2000; published 14 February 2001)

The melting and freezing of Ar condensed into a porous silica matrix (Vycor glass) has been investigated by heat capacity and vapor pressure measurements for various filling fractions and sample histories. A model is proposed which explains the reduction of the melting temperature, the thermal hysteresis between melting and freezing, and the shape and size of the melting and freezing anomaly in terms of interface melting in a cylindrical geometry. For incomplete fillings, freezing involves delayering transitions in particular of the third monolayer. The first and second monolayer on the pore walls do not participate in freezing and melting.

DOI: 10.1103/PhysRevB.63.104202 PACS number(s): 61.43.Gt, 64.70.Dv, 65.40.Ba

I. INTRODUCTION

It is well established by numerous studies that the melting point of van der Waals liquids (ranging from cryosystems such as H_2 to larger organic molecules)[1,2] and of hydrogen bonded systems (such as water[3–5]) embedded in pores is lower than in the bulk state. Furthermore there is considerable thermal hysteresis between melting and freezing and melting and freezing (at temperatures T_m and T_f, respectively) appear to evolve continuously as demonstrated by the width of the corresponding anomalies in heat capacity measurements. The freezing anomaly is usually somewhat sharper than the melting anomaly, but both occur below the triple point temperature T_3 of the bulk system, have a relatively sharp high-T cutoff and a long wing towards low T.[1] The reduction of the melting temperature scales with the inverse pore radius R, $T_3 - T_m \propto 1/R$.[3]

The finite T range of melting is usually attributed to the pore size distribution $\rho(R)$ of the matrix material,[6] Vycor glass being the most prominent one. The material in the narrow sections of the pore network is the last to freeze on cooling and the first to melt on heating. This opens the possibility of pore size spectroscopy. See, however, our critical comments in Ref. 7. Most authors have observed that the heat of fusion is lower than in the bulk and occasionally it has been reported that the heat of melting is larger than the heat released on freezing.[2,5] See, e.g., Molz *et al.*[8] for Ar and several other cryoliquids in Vycor. However, Molz *et al.* carefully point out that this apparent violation of the first law of thermodynamics must be an artifact of the employed technique, namely, ac calorimetry.

The pores are usually filled by simply letting the liquid penetrate into the matrix by capillary forces. In our recent studies of Ar,N_2,CO in porous glasses we prepared the pore fillings by condensation out of the vapor phase.[9,10] This has several advantages. Not only are the solid pore fillings of better crystallographic quality, but also fractional pore fillings f can be prepared in a controlled way and the vapor pressure p vs f isotherms give direct access to the chemical potential μ of the pore filling. The isotherms, both in the liquid (see Fig. 1) and the solid state, are at low f and p similar that what is obtained by adsorption on planar substrates, and are in fact well described by the BET model.[11,12] Hence there is no doubt that the first material offered to the porous matrix forms an adsorbate layer on the pore walls. At some critical value of f and p, capillary condensation occurs. Capillary condensation involves a qualitative change of the condensate-vapor interface and is hence a phase transition of first order with a hysteresis with respect to adsorption and filling (at vapor pressure p_f) and desorption and emptying (at p_e, $p_e < p_f$).[13] For a cylindrical pore, the condensate-vapor interface is of cylindrical shape for the adsorbate state of the pore filling at lower f whereas for the capillary condensate the interface forms a concave meniscus. The pores then fill and empty by a lateral motion of this meniscus along the pore. Under ideal conditions these processes should take place at constant p_f and p_e, respectively. The experimental isotherms show that this is approximately so for emptying, but the filling branch of the isotherms is smeared out, at least in the liquid state. There are reasons[9] to think that p_e (and not p_f) is close to the equilibrium pressure at which the capillary condensate in one part of the pore coexists with the vapor and the adsorbate of maximum thickness d_e in the other part. Therefore the difference of the chemical potential $\Delta\mu$ of the capillary condensate and of the bulk state is just given by $kT \ln(p_e/p_0)$. p_0 is the saturated vapor pressure. On adsorption, a metastable adsorbate film of a thickness d_f larger than d_e can be grown on the pore walls. Given the

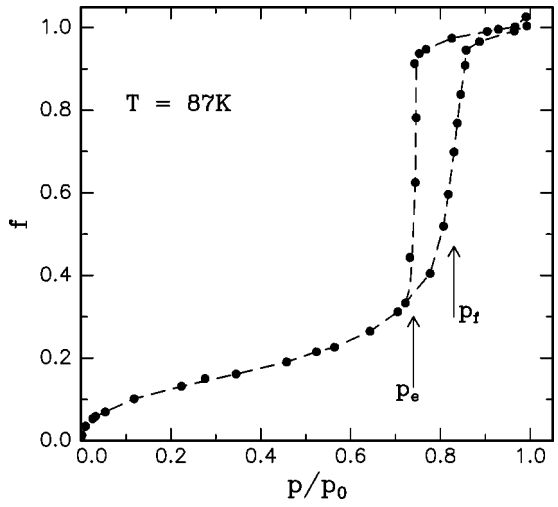

FIG. 1. Adsorption-desorption isotherm (fractional filling f vs reduced vapor pressure) in the liquid state at 87 K.

total wall area (from the BET analysis of the initial part of the f vs p isotherms), the pore volume (from the amount of material necessary for complete filling, $f=1$) and the size of the molecule, d_e and d_f can be obtained from the corresponding f values. For simplicity, we quote the thickness in monolayer equivalents ML. For Ar,N_2,CO in Vycor and SiO_2 xerogels with pore diameters ranging from 5 to 13 nm, we obtained values of $d_e^l=3$ ML, $d_e^s=2$ ML, $d_f^s=3$ ML. d_f^l is not well defined, but definitely much larger, a reasonable estimate is 5 or 6 ML.[9,10] Here l refers to the liquid and s to the solid state.

Assuming phase equilibrium of the liquid and the solid phase at T_3 for the bulk system and at T_m for the capillary condensate, T_3-T_m is related to the $\Delta\mu$'s via $T_3-T_m=(|\Delta\mu^l|-|\Delta\mu^s|)/\Delta S$. ΔS is the entropy of melting. Thus the depression of the melting temperature in the pores is related to the fact that $|\Delta\mu^s|<|\Delta\mu^l|$, which we have interpreted in the sense that the capillary condensate profits from the attractive wall potential in both the liquid and the solid crystalline state and hence forms a concave meniscus in both states, but that the solid has to allow for lattice defects in order to adapt to the pore geometry.[9] In more macroscopic terms $|\Delta\mu^s|<|\Delta\mu^l|$ means that the radius of curvature of the meniscus and the contact angle θ of the condensate-vapor interface with the pore wall are larger in the solid than in the liquid state. For the liquid state, it is usually assumed, explicitly or tacitly, that $\theta=0$ and that the radius of curvature is equal to the pore radius R which then leads to a $1/R$ dependence of $\Delta\mu$ (Kelvin equation). This also means that the narrow pores are the first to fill by capillary condensation on adsorption and the last to empty on desorption. More generally, the $1/R$ dependence results from the competition of a surface and a volume free energy.

Thus some aspects of pore melting are understood approximately, whereas others, the hysteresis, the heats of freezing and melting, as well as the peculiar shapes of the freezing and melting anomalies are not. Our study deals with Ar in Vycor. Ar is considered a very simple system, Vycor is a standard matrix material. Hence we think that our results and interpretations are representative at least for the whole family of van der Waals condensates in porous silica materials, but perhaps also for other combinations of filling and matrix.

II. EXPERIMENTAL

Some information on the experimental setup has been given previously.[7] We recall that we use Vycor glass (Corning, code 7930) as porous matrix, but that the present sample taken from a new batch of Vycor has an avarage pore diameter of about 10 nm instead of the usual 7 nm.

For a heat capacity measurement on first order phase transitions with thermal hysteresis, it is essential to change the temperature monotonously. Otherwise one can easily miss parts of the latent heat or get contributions from the melting and freezing of the same fraction of material more then once. We therefore used a scanning rather than the previously applied quasiadiabatic heat pulse technique. The heat capacity c is extracted from the heat flow dQ/dt at a given heating or cooling rate dT/dt, $c\propto(dQ/dt)/(dT/dt)$, $dQ/dt=Z\Delta T$, where Z is the heat leak and ΔT the temperature difference between the sample and the thermal shield. A typical value for ΔT is 0.25 K. The heat leak is realized by admitting some mbar of He gas into the space between the sample and the heat shield. We have not determined the value of Z, but rather calibrate the heat capacity derived with the scanning technique with the results obtained with the quasiadiabatic method. For the heating and cooling rate we have chosen 0.05 K/min, large enough to guarantee a sufficient quality of the heat capacity data and slow enough to maintain the thermal equilibrium between the vapor and the pore condensate at least approximately, as demonstrated by the vapor pressure data of Fig. 2 which are in good agreement with previous ones[7] which have been obtained by isothermal adsorption and desorption.

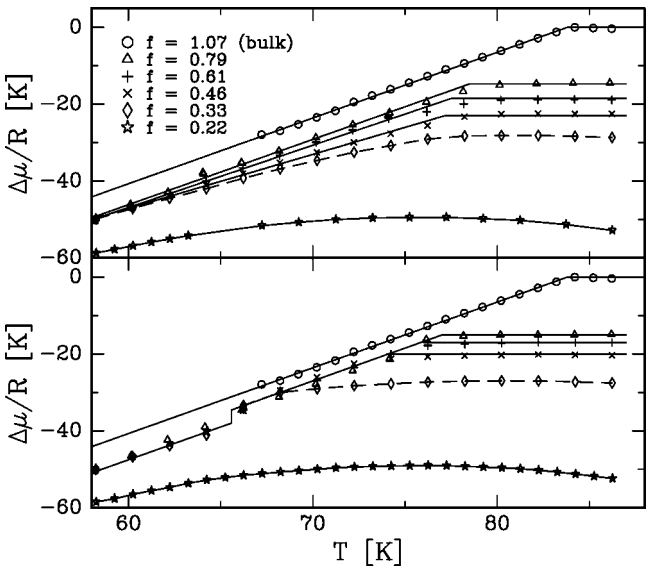

FIG. 2. Chemical potential vs temperature isosters as obtained by heating (upper frame) and cooling (lower frame) scans for a series of fractional fillings f prepared by adsorption at 87 K.

The pore fillings have been prepared by condensation of vapor at 87 K, a temperature well above $T_3=83.8$ K. We concentrate on samples for which the filling has been produced by adsorption, but also show a few results on samples where the pores have been filled completely and brought to the desired value of f by subsequent desorption. The adsorption-desorption 87 K isotherm is shown in Fig. 1. On cooling and heating the amount of material in the pores changes by adsorption out of and by desorption back into the vapor, but the change of f is less than 1% and occurs almost exclusively above T_m. This effect has been corrected for and the results shown for heating and cooling scans can be considered isosteric. Actually the samples have been thermally cycled at least twice between 87 and 60 K.

III. RESULTS

The heat capacity c versus T curves for a series of filling fractions is shown in Figs. 3 and 4 as obtained for first heating (after a first cooling down to 60 K) and for a second

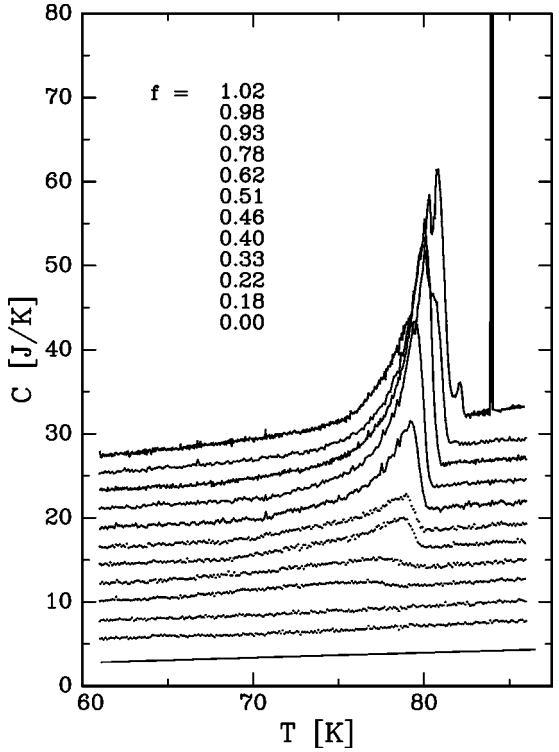

FIG. 3. Heating traces of the heat capacity c for several fractional fillings f. The curves are shifted upwards in steps of 2 J/K.

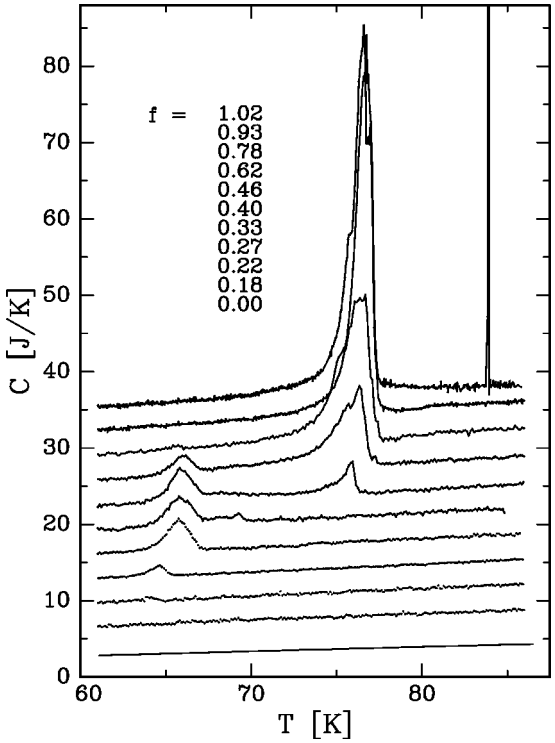

FIG. 4. Cooling traces of the heat capacity. The vertical offsets are 3 J/K.

cooling. The sharp spike showing up in slightly overfilled pores ($f=1.02$) is due to the melting and freezing of the bulk material outside the pores and hence is a marker for T_3. The heating curves match with those obtained previously with the heat-pulse technique. The general shape of the melting and freezing anomaly for $f\simeq 1$ is similar to what has been observed for many other systems confined in pores, see, e.g., Ref. 1. As pointed out already in our recent heat capacity study,[7] lower fillings which represent the adsorbate film on the pore wall do not show any anomalous contribution and hence do not undergo a melting phase transition. The anomalies are related exclusively to the capillary condensed material in the pore center.

Figure 5 shows the entropy of melting and of freezing ΔS, derived from the anomalous part of the heat capacity, as function of f. ΔS is proportional to $(f-f_c)S_0$, $f_c=(0.27\pm 0.03)$, the molar entropy of fusion S_0 is (14.2 ± 1) J/mol K, both on melting and freezing. The fraction f_c of the ''dead'' adsorbate layer on the pore walls corresponds to about 2 ML. The value of S_0 agrees with that of bulk Ar.[14] Normalizing ΔS to the total amount of Ar in the pores including the dead layer would of course yield a molar entropy and heat of fusion lower than for the bulk.

For freezing, ΔS includes the contribution $\Delta S'$ from the second anomaly around 66 K. The 66 K anomaly is an unexpected feature appearing at intermediate values of f, only. As function of f, the 66 K anomaly shows up for the first time slightly above f_c, is maximum around $f=0.40$ and decreases for higher f (Fig. 5). The amount of material, the freezing of which leads to the maximum value of this anomaly, is equivalent to about 1 ML.

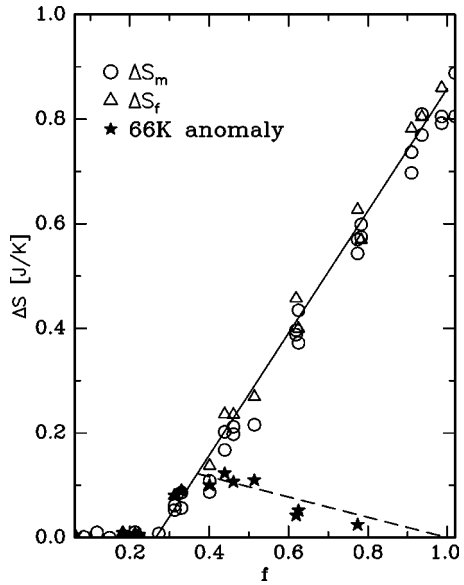

FIG. 5. The entropy of melting and freezing ΔS_m and ΔS_f, as a function of the fractional filling f, as derived from the anomalous part of the heat capacity results of Figs. 3 and 4. The contribution $\Delta S'$ of the 66 K anomaly is included in ΔS_f, but also shown separately. The solid line is the result of a linear regression, its slope gives the molar entropy of fusion of the capillary condensate. The dashed line in combination with the solid line at lower f is the entropy related to the 66 K anomaly on the basis of the model described in the text.

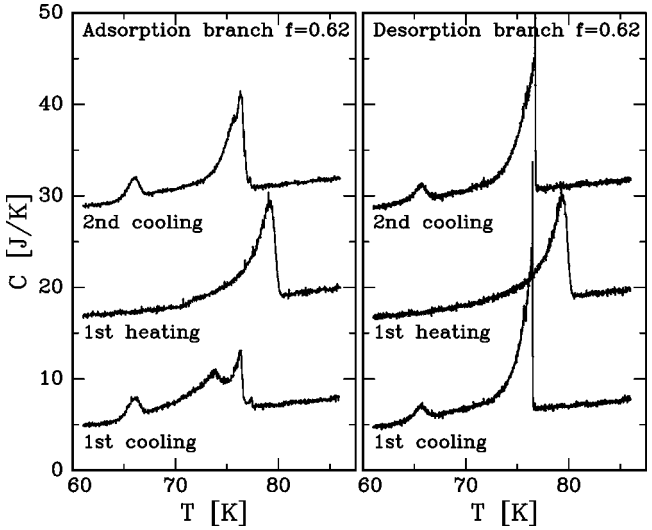

FIG. 6. The heat capacity for $f=0.62$ of the first cooling, the first heating, and the second cooling run. The second heating run (not shown) is identical to the first heating run. The left (right) panel refers to a sample prepared by adsorption (desorption) at 87 K.

Figure 2 shows the vapor pressure converted into $\Delta\mu$ as function of temperature for some selected values of f. The chemical potential of the bulk liquid is used as zero reference line. Such μ-T diagrams have been discussed in detail recently.[9] The chemical potential of the pore filling for any $f<1$ is lower than that of the bulk. Hence the pore fillings are stable with respect to the bulk state, both in liquid and solid form, even though $\Delta\mu$ is quite small. The μ-T isosters for $f>f_c$, show a more or less well defined change of slope which corresponds to the entropy ΔS of freezing and melting and hence determines the freezing and melting temperature of the capillary condensate in this type of experiment. ΔS and the characteristic temperatures agree well with the heat capacity results. The quasilinear sections of μ-T isosters are in general parallel to the corresponding sections of the bulk. Thus the entropy of the capillary condensate away from the melting/freezing transition is about identical to the bulk, both in the liquid and the solid state as already pointed out in Ref. 7.

For f values around 0.4, the μ-T isoster of the solid state shows a discontinuity at 66 K, which we interpret as a parallel displacement rather than a kink. This means that the 66 K anomaly of such fillings is due to the release of heat when the system transforms from a metastable state for 66 K$<T<T_f$ with a higher vapor pressure to the stable state below 66 K.

For $f=0.22$, that is for an adsorbate layer of about 2 ML on the pore walls, the μ-T-isoster bends over smoothly, without any apparent kink, from about parallel to the bulk solid at low T to about parallel to the bulk liquid at high T. Figure 6 shows results on hysteresis loops extending from 60 to 87 K, that is from a temperature well below the 66 K anomaly to a temperature well above T_m. Shown is $c(T)$, for the first cooling, the first heating and the second cooling scan for a sample with $f=0.62$ prepared by adsorption at 87 K as well as for a sample with the same value of f prepared by desorption at 87 K. The results are identical for both methods of preparation, except for first cooling.

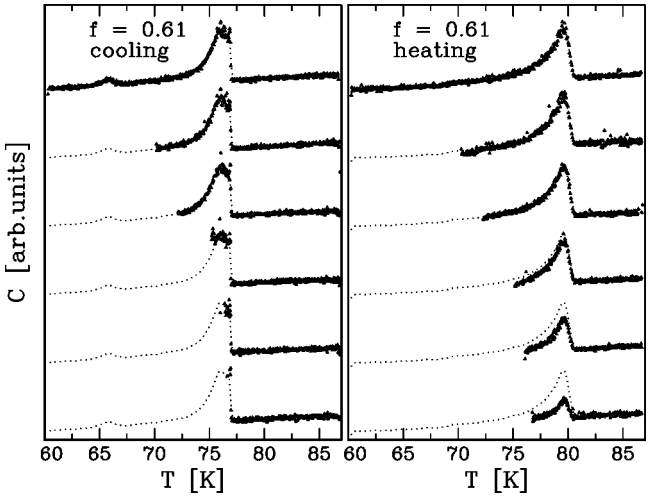

FIG. 7. Heat capacity results of $f=0.61$ for ''incomplete'' cooling-heating cycles. Cooling (left panel) starts at 87 K and stops at $T_{\min}$. Heating (right panel) brings the sample back to 87 K. $T_{\min}$ is varied from 60 K (top) to 77 K (bottom).

Figures 7, 8, and 9 show the results of ''incomplete'' thermal cycles. In Fig. 7 a sample with $f=0.61$ is cooled down from a temperature well above T_m to a temperature $T_{\min}$ and heated up again. In Figs. 8 ($f=0.61$) and 9 ($f=0.41$) heating starts at a temperature well below 66 K, brings the sample up to a temperature $T_{\max}$, whereupon the cycle is completed by recooling.

IV. INTERPRETATION AND DISCUSSION

Melting is a first order phase transition and hence involves a liquid-solid coexistence, interfacial energies, metastable states, and nucleation. In fact, there have been attempts to explain the thermal hysteresis of melting in pores

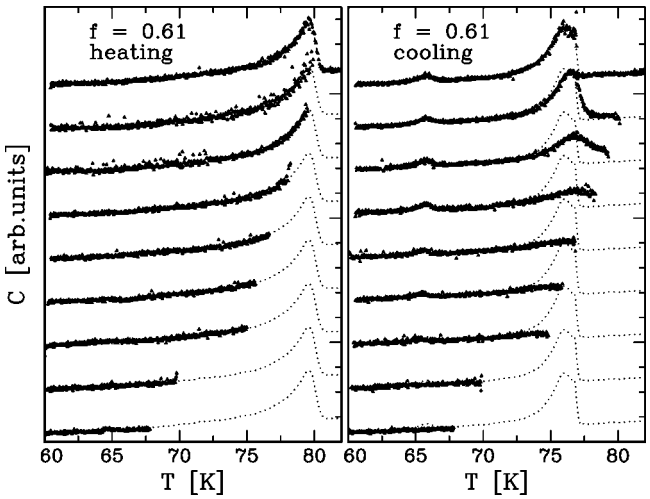

FIG. 8. Heat capacity results of $f=0.61$ for ''incomplete'' heating-cooling cycles. Heating (left panel) starts at 60 K and stops at $T_{\max}$. Cooling (right panel) brings the sample back to 60 K.

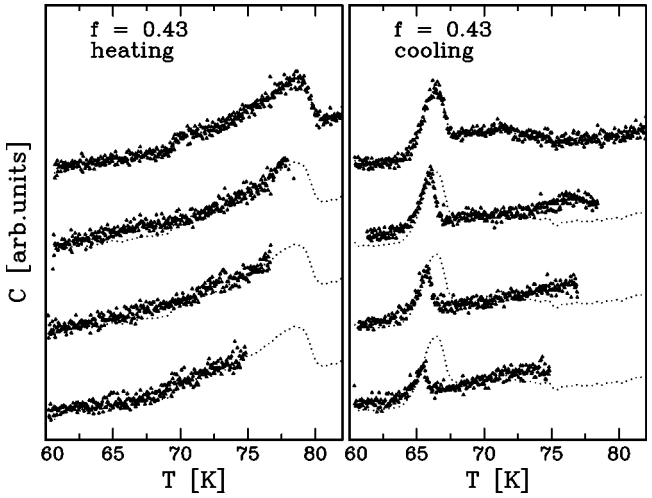

FIG. 9. Analogous to Fig. 8, but for $f=0.41$ or equivalently 3 ML.

by different shapes of the solid-liquid interface and of the critical nucleus, such as spherical or cylindrical.[15] It is also obvious that the pore size distribution is of relevance. In Ref. 7 we assumed independent cylindrical pores with different radii described by a Gaussian distribution $\rho(R)$. Starting out from $\Delta\mu$ and T_3-T_m being proportional to $1/R$, the asymmetric shape of the melting anomaly for $f=1$ could be explained qualitatively, but it turned out that the width of the distribution had to be chosen twice as large compared to what has been determined by small angle scattering and electron microscopy.[16]

Thermal equilibrium in completely filled pores

In the following we consider a homogeneous cylindrical pore. In case of a liquid-solid coexistence, the interface of the two phases is likely to be of cylindrical shape with one phase in the pore center and the other one next to the pore wall, either with the liquid or with the solid next to the wall.

The wall in this context is the pore wall coated with the dead layer of about 2 ML of Ar. The pore radius available for the active part of the pore filling is hence reduced to about 42 Å, instead of the nominal radius of about 50 Å. From the fact that $|\Delta\mu^s|<|\Delta\mu^l|$, one expects that the liquid can accommodate to the amorphous structure of the dressed wall much more easily than a crystalline fcc pore solid. In this situation the net interfacial energy $\Delta\gamma=\gamma_{ws}-\gamma_{wl}-\gamma_{ls}$ is expected to be positive[15] (''w'' for wall) and the pore filling can profit from the intrusion of a liquid shell between the wall and the solid in the pore center. See Fig. 10 for a schematic view of the pore cross section. Analogous views have been propagated for other first order phase transition at interfaces,[17] surface melting in particular[18] (where the surrounding medium is not the glass matrix but the vapor). For a cylindrical geometry it is essential to realize that—in contrast to planar interfaces—the area of the s-l interface and the l and s volume fraction depend on the distance r of this interface from the pore center. Correcting the energy functional of the planar geometry for this point, the free energy F_L per unit length of the pore is obtained as

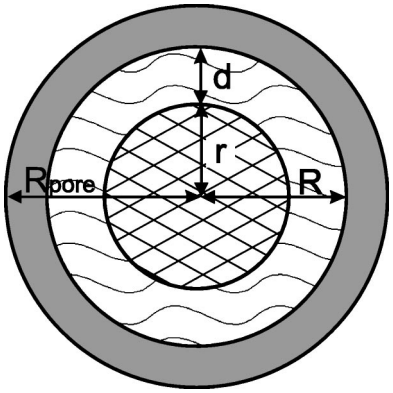

FIG. 10. Schematic view of the cross section of a completely filled pore at a temperature somewhat below T_0. Shaded: dead adsorbate layer, wavy: intruding liquid layer, cross hatched: crystalline material in the pore center.

$$F_L=\pi(R^2-r^2)L\frac{T_3-T}{T_3}+2\pi r\gamma_{ls}+2\pi R(\gamma_{wl}+\Delta\gamma e^{-d/\xi})$$

(see Ref. 19 for the spherical geometry). Here the first term is the difference of the volume free energies of the liquid and the solid, and the last term considers the fact that the order parameter of the solid phase can vary in space only smoothly. Thereby a coherence length ξ enters into the problem. d is the thickness of the liquid layer in contact with wall, r the radius of the solid core, $r+d=R$, and L the latent heat of fusion, $L=T_3\,\Delta S$. The dependence of F_L on r is shown in Fig. 11 for three temperatures. The equilibrium value $r_0(T)$ of r is given by the absolute minimum of F_L. The volume fraction f_l of the liquid corresponding to $r_0(T)$

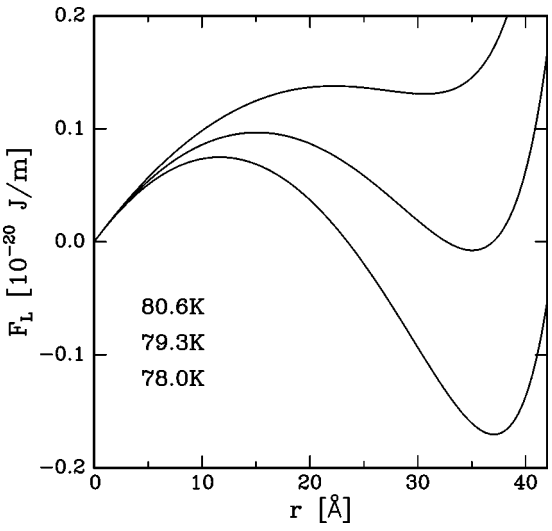

FIG. 11. The free energy F_L per unit length as function of the radius r of the solid core in the pore center for three temperatures, as calculated from the model described in the text. The individual curves have been shifted vertically in order to coincide for $r=0$. The value chosen for the coherence length ξ is 1 ML.

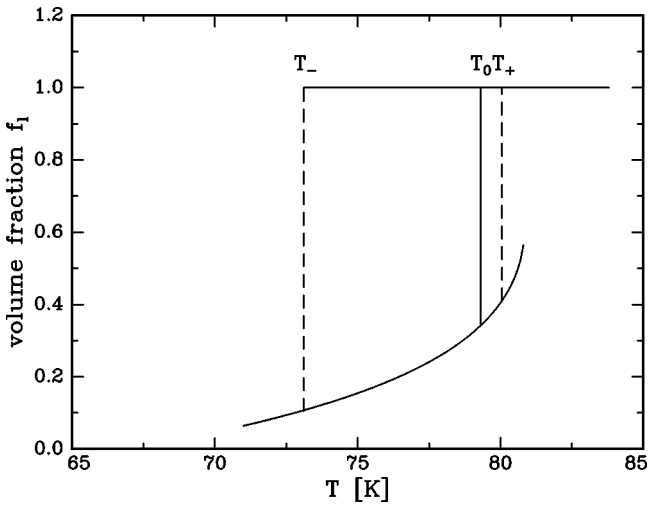

FIG. 12. The volume fraction f_l of the liquid as function of T, as calculated from the model (see text).

is shown in Fig. 12. Starting at low T, the liquid layer on the wall grows on heating. At some temperature $T_0<T_3$ a critical value r_c of r_0 is reached at which the remaining solid core in the pore center melts all at once. This happens when the release of energy due to the elimination of the *s-l* interface can compensate for the heat of fusion necessary for the melting of the residual solid in the pore center. This effect, a pecularity of the confined geometry, suppresses the divergence of thickness of the intruding liquid layer which would occur in planar geometry. There is also some analogy to capillary condensation where the growth of the adsorbate film is stopped and the vapor phase in the pore center is displaced by the condensate. Since the model is based on the competition of a volume and a interfacial energy, T_3-T_0 is proportional to $1/R$. The anomalous part of the heat capacity is obtained from Ldf_l/dT. There is a singular part, a latent heat of $L[1-f_l(r_c)]$ at T_0 and a nonsingular part, which shows up as a long tail at lower T, due to the growth of the intruding liquid layer.

Evidence for the existence of a liquid layer at temperatures well below the apparent melting temperature T_m is available not only from the low-T tail of the heat capacity anomaly, but also from NMR results on various pore fillings[20] which call for a mobile, liquidlike fraction of the pore filling at rather low T. We also think that the ultrasonic results of Molz *et al.* on Ar in Vycor[8] can be explained by such a liquid layer. These authors in fact mention that it appears that there is ''some liquid remaining at temperatures as low as 25 K,'' but later on propose that the peculiar behavior of the ultrasonic velocity and attenuation is not due to some residual liquid but to the thermally activated diffusion of vacancies within the solid.

Metastable states and hysteresis in completely filled pores

The free energy functional predicts a first order melting or freezing transition of the pore center at T_0 with inherent metastable states (Fig. 11). The solid core surrounded by the wetting layer can be superheated up to a temperature T_+, $T_0<T_+<T_3$ and the pore liquid can be supercooled down to T_-, $T_-<T_0$. Thus a natural explanation of the hysteresis between freezing and melting is supplied. The model in its present form actually suggests unrealistically low values of T_-. Note, however, that the minimum of $F_L(r)$ at $r=0$ which represents the supercooled liquid is only marginally stable at low T. Obviously (and not surprisingly) the model does not describe a very thin cylindrical solid core in the pore center correctly. Quite generally spinodal temperatures of mean field models are of little significance, because thermal fluctuation and heterogeneous nucleation usually reduce the range of metastability in real systems. Therefore we feel justified to calculate ''effective'' values of T_+ and T_- from the following *ad hoc* assumption. At the equilibrium temperature T_0 the free energy barrier between the coexisting states has a certain value $E_b(T_0)$, see Fig. 11. We then simply assume that the metastable states disappear at those temperatures for which the barrier $E_b(T)$ from the metastable state to the stable state is reduced to some fraction x of $E_b(T_0)$. The results on f_l including metastable states as calculated with $x=0.43$ are also shown in Fig. 12. The location of T_+ and T_- with respect to T_0 is asymmetric, T_+-T_0 being much smaller than T_0-T_-. Furthermore there is a more fundamental asymmetry between the metastable states of cooling and heating. It is only on cooling that the new phase has to nucleate, namely, in the pore center. On heating the liquid already exists as shell at the pore walls everywhere in the pore network and the *l-s* boundary just has to move forward for the pore filling to melt completely. For a cylindrical geometry the model shows that there is an energy barrier for the radial motion of the *l-s* boundary towards the pore center, but this is not necessarily so for other geometries. We think in particular of pores with a blind end. Here the *l-s* boundary can move out of the blind end along the pore axis without having to overcome a barrier. Hence the metastable states predicted for superheating are irrelevant. The pore fluid can be supercooled, but the pore solid cannot be superheated. In the following we therefore identify the phase equilibrium temperature T_0 with the melting temperature T_m and the lower spinodal temperature T_- with the freezing temperature T_f.

For a comparison with the experimental data it is necessary to choose a suitable pore size distribution $\rho(R)$ and to decide whether pores of different diameter freeze and melt independently or not.

A calculation of the freezing and melting anomaly for a Gaussian distribution $\rho(R)$ of independent pores is shown in Fig. 13. The parameters [$R_{\rm pore}=50$ Å, the variance of the distribution $\sigma=10$ Å, $\gamma_{ls}=2.1$ dyn/cm, $\Delta\gamma=1.9$ dyn/cm, $\xi=4.1$ Å (1 ML), and T_3,L,x as given above] have been chosen in a way to obtain agreement with the experiment for the melting anomaly and for the onset of freezing. Clearly the calculated freezing anomaly is much too broad.

How can it happen that the freezing peak is narrower than the melting peak? For freezing we abandon the idea of independent pores and refer to coupled pores in the following sense [for ease of discussion let us assume that $\rho(R)$ extends from $R_{\rm min}$ to $R_{\rm max}$]. On cooling, solidification should occur first in the center of the largest pore at $T_-(R_{\rm max})$. If the pores

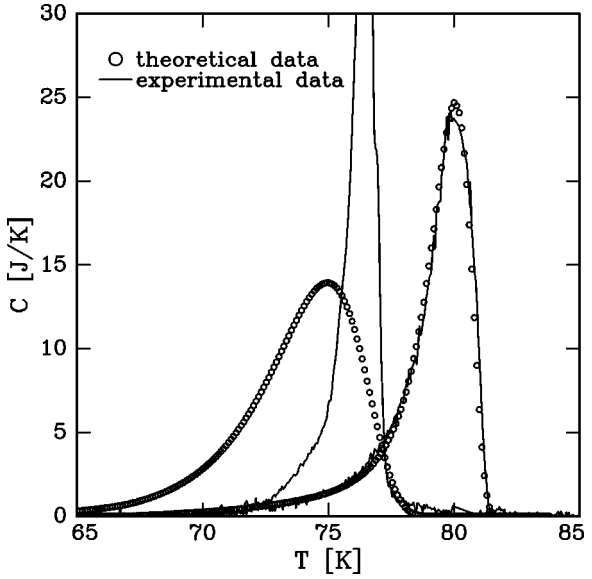

FIG. 13. The freezing and melting anomaly of the heat capacity both of the experiment ($f=0.93$, continuous curves) and of the model (circles). The parameters of the model and of the Gaussian distribution of the diameters of independent pores have been chosen in a way to obtain agreement for the melting anomaly and for the onset of freezing.

are now coupled, this solid acts as nucleus for solidification and eliminates metastable supercooled states in the centers of all narrower pores for which $T_0(R)$ is larger than $T_-(R_{\max})$. This should give rise to a δ-like heat capacity signal at $T_-(R_{\max})$. On further cooling the centers of the remaining pores then solidify at their individual equilibrium temperatures $T_0(R)$. Thus the freezing temperatures are spread out over a T interval the width of which is given by $\Delta_f = T_-(R_{\max}) - T_0(R_{\min})$. This has to be compared with the T interval of melting $\Delta_m = T_0(R_{\max}) - T_0(R_{\min})$. Δ_f is smaller than Δ_m. If $T_-(R_{\max}) < T_0(R_{\min})$, which means large thermal hysteresis and narrow pore size distribution, the centers of all pores freeze at a single temperature, namely, $T_-(R_{\max})$. The present system appears to be close to this latter case, since not only the freezing anomaly is relatively sharp, but also there is little overlap of the freezing and the melting anomaly (Fig. 13).

The results on the ''incomplete'' thermal cycles support these ideas. Figure 7 shows results obtained by cooling from a high temperature T, $T > T_m$ down to a temperature $T_{\min}$ and subsequent heating. The heating traces always show the same well defined endpoint of melting independent of the actual value of $T_{\min}$. This means that irregardless of how much material is actually solidified on cooling, melting always is completed at $T_0(R_{\max})$. Only the size of the melting anomaly depends on the fraction of material (in the larger pores) which has been solidified previously on cooling down to $T_{\min}$ and which then remelts on heating. In Fig. 8 the sample is heated up from a low temperature T, $T < T_f$, to a temperature $T_{\max}$ and recooled afterwards. This time the onset of freezing does depend on $T_{\max}$. If $T_{\max}$ is above the endpoint of melting $T_0(R_{\max})$, all material is liquified and hence solidification on subsequent cooling starts at $T_-(R_{\max})$. If on the other hand $T_{\max}$ is lower than $T_0(R_{\max})$, the material in the narrower sections of pore network which has been liquified by heating up to $T_{\max}$, directly solidifies on cooling at the individual equilibrium temperatures $T_0(R)$ because of the persistence of solid in the larger pores which then acts as nucleation center for solidification in the narrower pores. [Note that these experiments have been carried out for $f=0.61$, and not for $f=1$. Hence $R_{\max}$ should not be identified with maximum pore radius of $\rho(R)$ but with the radius of the largest pore which is actually occupied.]

Incomplete thermal cycles on the melting of pore fillings in Vycor had been studied previously by Molz *et al.* These authors summarize their heat capacity results on O_2 and the ultrasonic results on Ar by saying that freezing is extremely irreversible, whereas melting is more nearly reversible. This is consistent with our ideas.

Partially filled pores

For fractional fillings f, $f_c < f < 1$, the temperatures of maximum heat capacity as well as the high-T cutoffs of the anomalies shift to slightly lower values. This is readily explained by the $1/R$ dependence of the melting temperature in combination with the fact that for $f<1$ not all but only the pores up to some maximum value of the pore radius R are occupied. Surprising features are the appearance of the 66 K anomaly on cooling and the dependence of the heat capacity of the first cooling run on the sample preparation.

As pointed out above, the entropy $\Delta S'$ related to the 66 K anomaly is maximum for $f=0.4$ where it corresponds to the entropy of freezing of about 1 ML. For f around 0.4 which is equivalent to about 3 ML, freezing thus occurs at 66 K, a temperature well below the main freezing anomaly of the higher fillings. Melting for $f=0.4$ on the other hand is as expected. It takes place between 75 and 79 K, that is in the lower-T part of the melting anomaly as observed at higher fillings. This is documented not only by the results of shown in Figs. 3 and 4, but also by the ''incomplete'' heating-cooling cycles of Fig. 9: After heating up to $T_{\max} > 80$ K, the 66 K anomaly of the subsequent cooling run is fully developed. For lower values of $T_{\max}$ the size of the 66 K anomaly is reduced. After heating up for example to $T_{\max}=75$ K (lowest curve of Fig. 9), the 66 K anomaly has about one quarter of its original size, only. Thus the material which freezes at the anomalously low temperature of 66 K, melts somewhere around 75 to 80 K. For the 66 K anomaly to show up on freezing, it is necessary that the material involved starts out as liquid.

As mentioned in the Introduction, the adsorption-desorption isotherms show that the maximum filling fraction f_c of the adsorbate on the pore walls at which capillary condensation sets in is equivalent to 3 ML in the liquid state, but only equivalent to 2 ML in the solid state. The values quoted refer to stable adsorbate layers, as obtained by desorption. Accordingly cooling must eventually remove the third adsorbed fluid layer and convert it into solid capillary condensate. This is a delayering transition. We think that the 66 K anomaly is due to such a transition. The peculiar dependence of $\Delta S'$ on f can be explained in terms of the third layer in the

''empty'' part of the pore network, only. Assuming that the third layer delayers and freezes at 66 K independent of whether there is solid capillary condensate in the rest of the pore or not, $\Delta S'$ should be proportional to $(f-f_c)/(0.4-f_c)$ for $f_c<f<0.40$ and to $(1-f)/(1-0.4)$ for $0.40<f<1$. This type of f dependence is indicated in Fig. 5. The experiment is in reasonable agreement with this assumption.

According to this view, freezing in a partially filled pore proceeds as follows. The liquid capillary condensate in the filled part of the pore freezes at temperatures around 76 K, the third layer in the empty part, however, remains liquid down to 66 K where it delayers and joins the solid capillary condensate.

The same type of process, in particular in connection with ''triple point wetting,'' is very common in adsorbed multilayers on planar substrates. Here the nth liquid monolayer delayers and solidifies as bulk solid at some temperature T_n below T_3, for van der Waals interactions between the adsorbate molecule and the substrate T_3-T_n is proportional to n^{-3}. Delayering and solidification occurs when the layer line of the μ-T diagram, usually parallel to vapor-bulk liquid coexistence line, intersects the vapor-bulk solid coexistence line.[21] In fact the μ-T diagram for cooling of Fig. 2 is reminescent of such multilayer phase diagrams, the capillary condensate playing the role of the bulk state.

Delayering involves solidification, as pore solid in the present case, and is a phase transition of first order. Thus there should be a thermal hysteresis between delayering/freezing and layering/melting. On heating the 66 K anomaly is absent, the melting of the material which originally formed the third layer contributes to the melting anomaly of the capillary condensate. The third liquid layer is reestablished upon melting of the pore filling.

This interpretation suggests that there are three different arrangements of the material in the pores (see Fig. 14). On heating, the intermediate state with the third liquid layer coexisting with the solid capillary condensate is bypassed. The intermediate state accessible on cooling, only, must be metastable since its vapor pressure is higher and its μ-T isoster is offset to higher values compared to the reference state obtained by heating where the third layer is absent (Fig. 2).

In the liquid regime ($T>T_m$) pore emptying leaves behind a stable adsorbate film the maximum thickness of which corresponds to 3 ML. On adsorption the adsorbate layer on the pore walls can be grown to a somewhat larger critical thickness of about 5 or 6 ML, all ML beyond the third one are metastable and are removed if once capillary condensation has occurred. The results of cooling and heating cycles on samples with $f=0.62$ as prepared by adsorption and desorption in the liquid regime are shown in Fig. 6. The sample prepared by adsorption consists initially of about 5 ML on the pore wall. The first cooling trace of this sample shows—in addition to the 66 K anomaly—a main freezing anomaly which is actually split into two (possibly even three) components. All other cycles are as expected and independent on the sample history. Hence we propose to relate the components of the split freezing anomaly of the first cooling run to the simultaneous process of delayering and conversion into solid capillary condensate of the fourth and fifth (and perhaps traces of the sixth) metastable fluid monolayer in very much the same way as this happens for the third stable fluid layer at 66 K. In contrast to the third layer, the metastable higher layers are of course not restored on heating back into the liquid regime. This view is supported by the shape of the μ-T diagram as obtained for cooling (Fig. 2). See the μ-T lines for $f=0.61$ and the neighboring f values of 0.46 and 0.79.

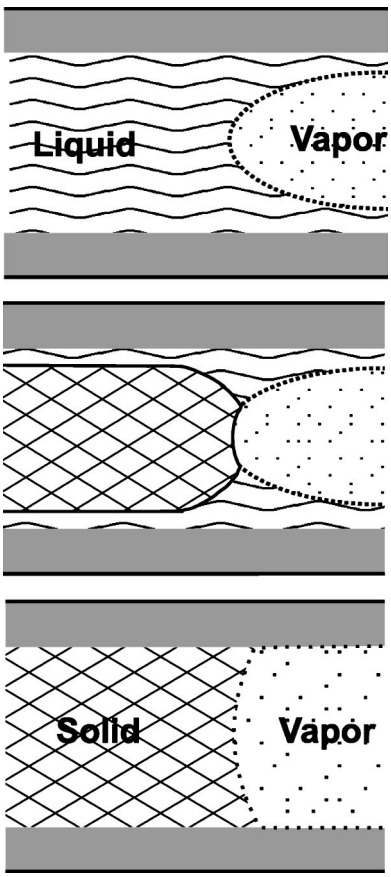

FIG. 14. Schematic picture of the three different types how the pore material organizes itself in a partially filled pore. The arrangement at the top refers to the liquid state, that at the bottom to the solid state at very low T. On cooling the metastable arrangement, shown in the center, exists in a T interval ranging from T_f (about 76 K) to 66 K.

Discrete adsorbed layers in porous glasses are unexpected. The atomically rough walls of the glass matrix and variations of the pore radius have been thought to smear out any signature of discrete monolayers. Indeed, even the best examples of vapor pressure adsorption isotherms fail to show such steps. On the other hand, one may argue that the dead layer on the pore walls smoothes the walls, and that the heat capacity (as a second derivative of the free energy) is more sensitive a probe than the vapor pressure (as a first derivative) in particular if the heat capacity signal is enhanced by the anomalous response at a first order phase transition.

V. SUMMARY

Our study has shown that the latent heats of freezing and melting in nanopores are identical with the heat of fusion of

the bulk state when referring properly to the mobile part of the pore filling, that is to the material in excess to a dead adsorbate layer of about two monolayers on the pore walls.

The reduction of the melting temperture with respect to the bulk, the long low-T tail of the heat capacity anomaly and the thermal hysteresis between freezing and melting can be explained by the concept of melting at interfaces adapted to the cylindrical pore geometry: A quasiliquid ''wetting'' layer intrudes between the wall and the solid core, grows on heating and finally leads at some critical thickness to the melting of the residual solid in the pore center. The hysteresis is due metastable states connected with this latter first order transition.

According to the Clapeyron equation cited in the Introduction, the reduction of the melting temperature is related to the fact that $|\Delta\mu^l|>|\Delta\mu^s|$. Previously we had to resort to lattice defects in order to account for this inequality, the present model supplies a perhaps somewhat more elegant geometric interpretation in terms of interfacial energies.

The shape of the freezing and melting anomaly, the freezing anomaly being sharper than the melting anomaly, and the peculiar freezing and melting behavior as observed in incomplete thermal cycles supply strong evidence that the melting takes place at the equilibrium phase transition temperatures $T_0(R)$ of the individual pores. On cooling, however, the metastable state of the supercooled liquid is of importance. The solid occurring first in the widest pore acts as nucleus for the freezing of narrower pores. This gives rise to a relatively sharp freezing anomaly of the heat capacity, despite of a relatively broad pore size distribution.

For fractional pore fillings, heat capacity anomalies arising from individual adsorbed monolayers residing in those parts of the pore network which are not filled with capillary condensate have been detected. Such layers show delayering and freezing transitions on cooling where they convert into solid capillary condensate and melt as such on subsequent heating. The third monolayer is reestablished on melting, higher layers, which are instable with respect to desorption, are not.

Thus melting and freezing in pores is quite complex a process, but the major ingredients, namely, the change of the character of a first order phase transition when evolving at a wall, the elimination of an interface due to the confined geometry and layering and delayering are well established concepts in other fields of condensed matter physics.

ACKNOWLEDGMENTS

This work has been supported by the Sonderforschungsbereich 277.

[1] J.L. Tell and H.J. Maris, Phys. Rev. B **28**, 5122 (1983).
[2] C.L. Jackson and G.B. McKenna, J. Chem. Phys. **93**, 9002 (1990).
[3] G.K. Rennie and J. Clifford, J. Chem. Soc., Faraday Trans. 1 **73**, 680 (1976).
[4] K. Morishige and K. Kawano, J. Chem. Phys. **110**, 4867 (1999).
[5] G.G. Litvan, Can. J. Chem. **44**, 2617 (1966).
[6] M. Brun, A. Lallemand, J.F. Quinson, and C. Eyraud, Thermochim. Acta **21**, 59 (1977).
[7] D. Wallacher and K. Knorr, J. Phys. IV **10**, Pr7-151 (2000).
[8] E. Molz, A.P.Y. Wong, M.H.W. Chan, and J.R. Beamish, Phys. Rev. B **48**, 5741 (1993).
[9] P. Huber and K. Knorr, Phys. Rev. B **60**, 12 657 (1999).
[10] P. Huber, D. Wallacher, and K. Knorr, Phys. Rev. B **60**, 12 666 (1999).
[11] S. Brunauer, P.H. Emmett, and E. Teller, J. Am. Chem. Soc. **60**, 309 (1938).
[12] S.J. Gregg and K.S.W. Sing, in *Adsorption Surface Area, and Porosity* (Academic, New York, 1967).
[13] W.F. Saam and M.W. Cole, Phys. Rev. B **11**, 1086 (1975).
[14] P. Flubacher, A.J. Leadbetter, and J.A. Morrison, Proc. Phys. Soc. London **78**, 1449 (1968).
[15] K.M. Unruh, T.E. Huber, and C.A. Huber, Phys. Rev. B **48**, 9021 (1993).
[16] P. Levitz, G. Ehret, S.K. Sinha, and J.M. Drake, J. Chem. Phys. **95**, 6151 (1991).
[17] D. Beaglehole, J. Cryst. Growth **112**, 663 (1991).
[18] D. Zhu and J.G. Dash, Phys. Rev. Lett. **57**, 2959 (1986).
[19] R.R. Vanfleet and J.M. Mochel, Surf. Sci. **341**, 40 (1995).
[20] K. Overloop and L. Van Gerven, J. Magn. Reson., Sec. A **101**, 179 (1993).
[21] G.B. Hess, in *Phase Transitions in Surface Films 2*, edited by Taub *et al.* (Plenum Press, New York, 1991).